JOURNAL OF MATERIALS SCIENCE 33 (1998) 2305–2312

Atomic force microscopy on tree-like crystals in polyvinylidene fluoride blends

K. CRÄMER, M. FOGLIATO SANTOS LIMA*, S. N. MAGONOV
Freiburger Materialforschungszentrum (FMF), Albert-Ludwigs University, Stefan-Meier-Strasse 21, D-79104 Freiburg, Germany
E. H. HELLMANN, M. JACOBS, G. P. HELLMANN‡
Deutsches Kunststoff-Institut (DKI), Schlossgartenstrasse 6, D-64289 Darmstadt, Germany
E-mail: ghellmann@dki.tv-darmstadt.de

Polyvinylidene fluoride (PVDF), in homogeneous blends with an amorphous polymer under specific conditions, forms crystals with a tree-like architecture. Tree-like crystals have a loose fractal structure of crystalline branches which are impregnated with the amorphous polymer. In a previous study, this spectacular morphology was investigated in blends of PVDF and a random copolymer of styrene and methylmethacrylate (SMMA, 13% wt/wt styrene) by light microscopy. The crystal growth was interpreted in terms of a rate competition of crystallization and interdiffusion. The submicroscopic structure of tree-like PVDF spherulites has now been characterized by atomic force microscopy. Surface profiles were prepared by etching PVDF/SMMA blend films with toluene. The tree-like spherulites proved to be less disordered than expected. Their core consists of a compact array of lamellae, the planes of which are periodically twisted, producing a ring pattern. Near the crystallizing front, branches grow, separated from each other, into the amorphous phase. They are internally as compact as the core, but are covered by a loose fur of disordered lamellae. The tree-like appearance of these crystals comes from frequent splitting of the branches into twigs. Crystallographic bifurcation as in dendritic crystals was not observed. At interfaces between two tree-like crystals, the lamellae form patterns of backfolding.

1. Introduction

When growing in homogeneous blends, polyvinylidene fluoride (PVDF) crystals can develop spectacular structures, as shown in Fig. 1 [1–6]. From their growth mechanism, these lofty crystals must be classified as spherulites, but they have a particular problem in that the blend melt contains, besides PVDF, another polymer that cannot crystallize. In Fig. 1, this is an atactic random copolymer $S_{13}MMA_{87}$ of styrene and methylmethacrylate (SMMA). Molten PVDF and SMMA are miscible on a molecular scale. Crystallization in blend melts from a molten mixture of PVDF and SMMA, was discussed elsewhere [1].

In these blend melts, growing crystals incorporate only PVDF chains but reject SMMA chains. Evidently, the amorphous polymer must concentrate somewhere. This controls the morphology of the crystals. Particularly interesting are the cases indicated in Fig. 2 where the crystallization and chain diffusion proceed at similar rates. In Fig. 2a, a compact PVDF spherulite grows into the melt. The amorphous SMMA chains escape from the advancing front by diffusion and form a halo (or depletion layer) around the crystal. In this halo, the PVDF concentration is low (depleted). In Fig. 2b, the chain diffusion is somewhat slower than the crystallization, which is thus hindered. This destabilizes the growth of a compact spherulitic front. Instead, the PVDF crystal produces branches that extend into the melt, sometimes bifurcating, and the amorphous SMMA is incorporated into the crystal, between the branches and twigs of an open tree-like architecture.

The compositions and temperatures where tree-like PVDF crystals are observed are indicated in the phase diagram in Fig. 3. The rates of crystallization and diffusion are properly balanced only in a confined region of the diagram extending from lower left to upper right (for details, see [1]).

PVDF crystallizes normally in two modifications, classified as α and γ. As shown in Fig. 4. the two are easily distinguished by their habit when grown in dilute solution [7, 8]. In the melt of pure PVDF, however, α and γ can look very similar [9–12], but in blend melts as PVDF/SMMA, the two are again easily distinguished because only the α modification

---

[*] On leave from the Institute of Chemistry-UFRGS, Porto Alegre, Brazil.
[‡] Author to whom all correspondence should be addressed.

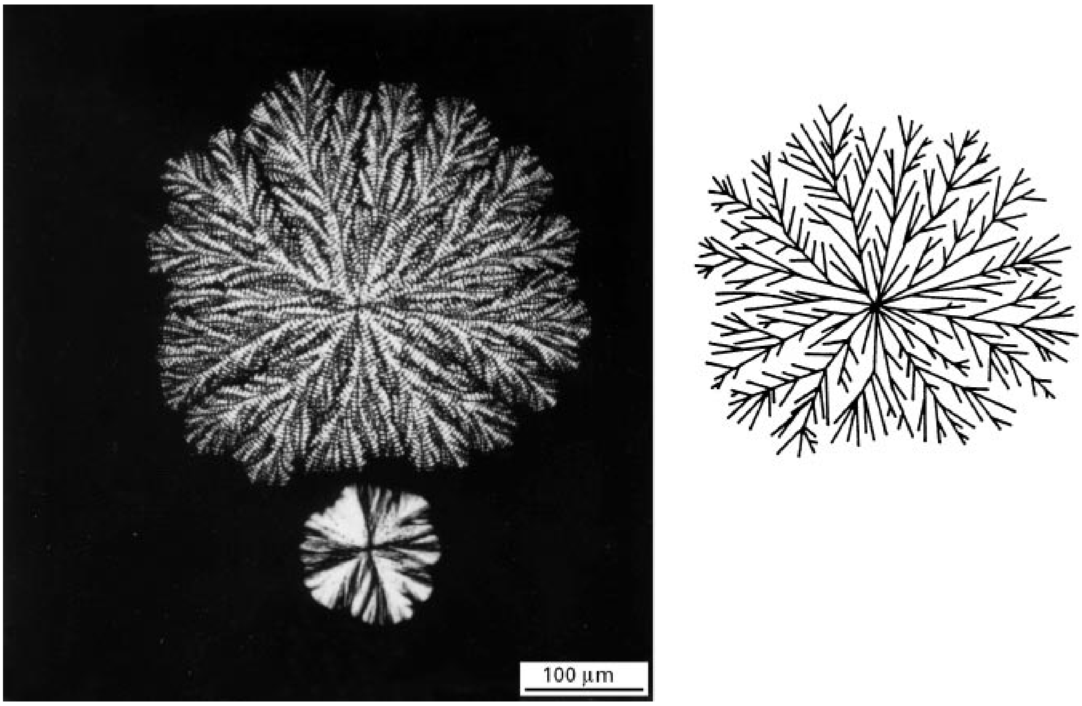

Figure 1 A tree-like α spherulite (large) and a γ spherulite (small) of PVDF in a homogeneous PVDF/SMMA blend [1].

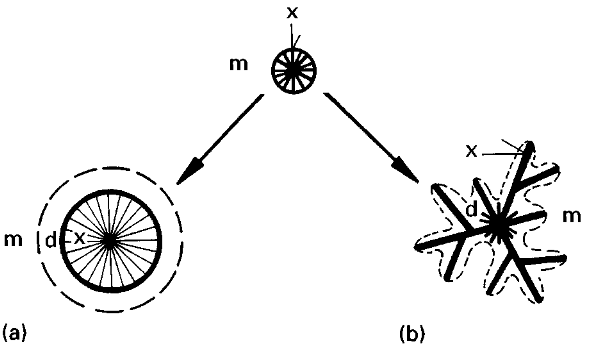

Figure 2 Crystallization in blends: while the nucleus of a crystal (x) grows in a blend melt (m), it ejects the amorphous component which forms depletion zones (d); (a) fast diffusion leads to a compact spherulite surrounded by a depletion halo, (b) slower diffusion leads to a tree-like architecture of branches and twigs with built-in depletion zones.

grows in a tree-like fashion. This is particularly obvious in Fig. 5, which shows a completely crystallized PVDF/SMMA blend with tree-like α and compact γ spherulites. Light micrographs such as Fig. 5 were the topic of a previous report [1]. Here, the crystals are discussed on a submicroscopic scale, on the basis of atomic force microscopy (AFM) [13–15].

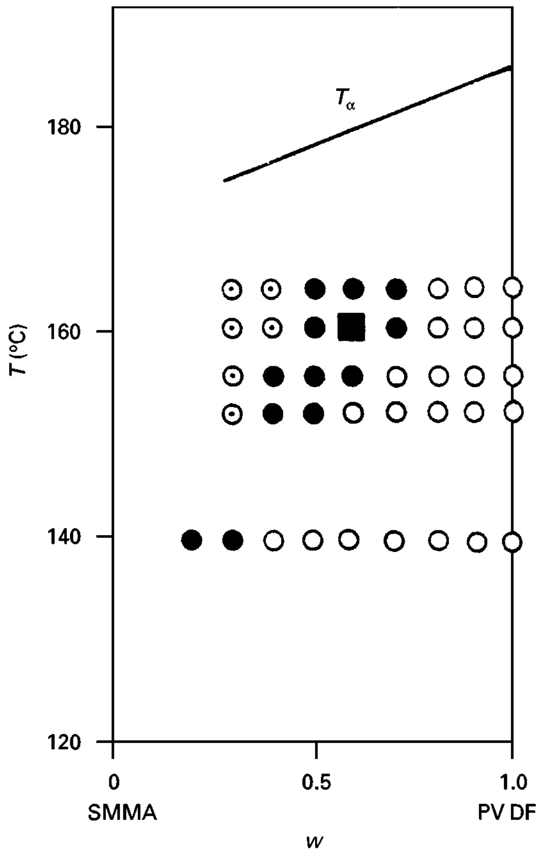

Figure 3 Phase diagram of the PVDF/SMMA blend system indicating α crystal morphologies [1]: (●) tree-like or (○, ⊙) compact spherulites; *w*, PVDF fraction; T_α, melting point.

2. Experimental procedure

The PVDF was Solef 1008 from Solvay ($M_\mathrm{w} = 100 \times 10^3$, $M_\mathrm{w}M_\mathrm{n} = 2.5$) with 4 mol % head-to-head linkages. The copolymer SMMA was prepared by free-radical polymerization, to low conversion in order to keep the composition (13 wt%/wt styrene) constant ($M_\mathrm{w} = 174 \times 10^3$, $M_\mathrm{w}/M_\mathrm{n} = 1.6$). The blend PVDF/SMMA with a weight ratio of 3: 2 was prepared by slowly casting a film from γ-butyrolactone solution on glass at 120 °C under nitrogen. The film, 80 μm thick, had DSC melting points at 179 °C (α) and 188 °C (γ modification of PVDF). It was heated for 30 min to 200 °C, cooled for crystallization for 12 d at 161 °C, and then quenched rapidly to room temperature.

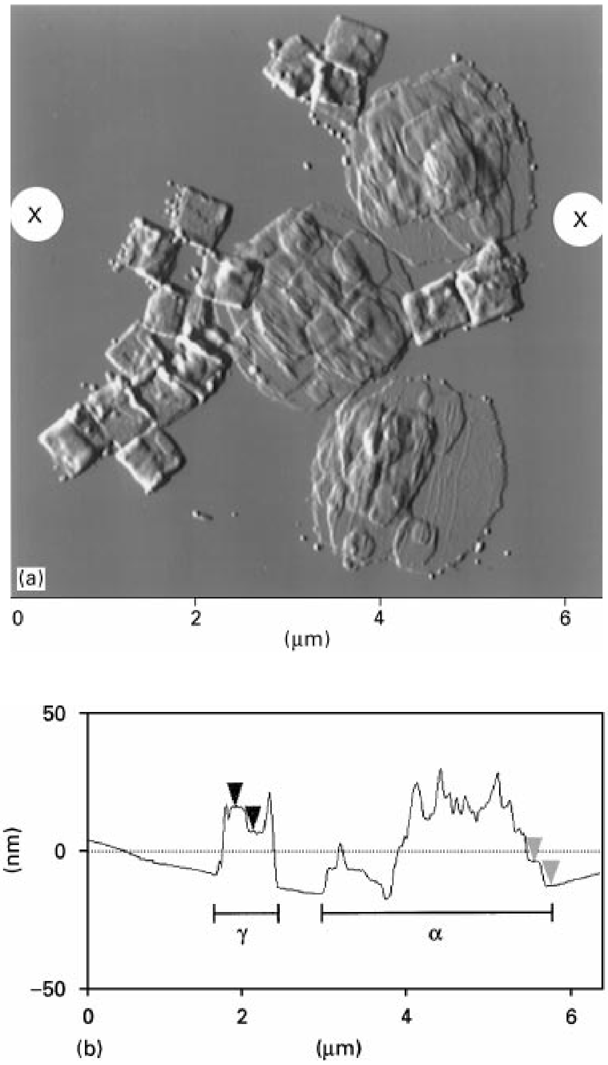

Figure 4 (a) AFM image (deflection) of single crystals of the α (hexagons) and the γ modification (squares) from 0.01% solution, with (b) a height profile along the line X–X.

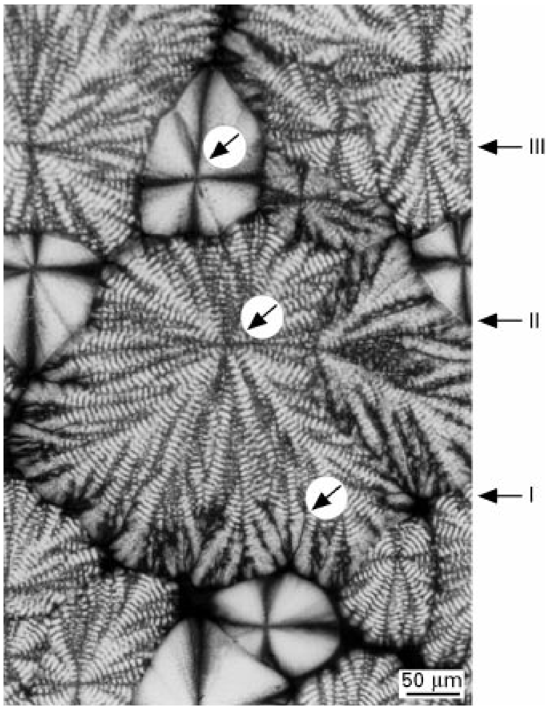

Figure 5 Light micrograph of the blend PVDF/SMMA (3 : 2 wt/wt), crystallized at 161 °C. The α and γ crystals were studied by AFM at the indicated sites; arrow I (Figs 6, 7), arrow II (Figs 9a, b, 10, 11), arrow III (Fig. 9c, d).

For the light micrographs, an Olympus Vanox AH2 Research Microscope was used. The pictures were taken under crossed polarizers.

For AFM, the film was immersed for 20 min in toluene at room temperature to etch away the SMMA. Etching was necessary because in unetched films, the top surface was rougher (height variations $\Delta h \leqslant 1$ µm) than the interface with the glass at the bottom ($\Delta h \leqslant 0.1$ µm) but the crystals were buried in the amorphous SMMA and were almost invisible. After etching, the roughness on both sides was $\Delta h \leqslant 1$ µm but the characteristic morphologies emerged. These structures are presented below. To test for artefacts, the etching time was reduced. Throughout, the same results were obtained, but with an inferior quality.

Ambient conditions and underwater AFM measurements were performed in the contact mode with a scanning probe microscope, Nanoscope III (Digital Instruments Inc.). Rectangular silicon cantilevers ("Nanoprobes") were used with force constants of approximately 0.1 $\mathrm{N\,m^{-1}}$ supplied by the microscope manufacturer. For the large-scale (small-scale) images, a *J*-scanner (*D*-scanner) was applied that allows scanning of areas up to $100 \times 100 (17 \times 17)\,\mu\mathrm{m}^2$. The contact imaging was conducted in the constant-force mode with high feedback gains. Height and deflection images were recorded simultaneously. The surface corrugation is correctly reproduced by the height image ("mountains" appear bright, "valleys" dark). The deflection image presents basically the height derivatives. Gradients are measured, not the absolute heights. The deflection image provides better resolution of nanoscale details because it focuses on steps and slopes. Further experimental details for the AFM measurements are described elsewhere [16]. The following section gives details of the type of image (height, deflection) and the range of height variation, Δh.

The basic difference of the contrast in light and AFM micrographs must be recognized. Optical transmission microscopy on crystals owes its contrast to the birefringence of the oriented, optically anisotropic crystal lamellae which are viewed in transmission, whereas AFM reveals the topographical height pattern on the surface of the film.

3. Results

Fig. 4 shows single crystals of α and γ PVDF that were grown on mica from a dilute chlorobenzene/DMF solution (0.01 wt %) by slow cooling from 140 °C [17]. The steps in the height profile in Fig. 4 yield for both α and γ single lamellae a thickness of 8 ± 2 nm, which exceeds the estimate from transmission electron microscopic shadows, $\cong 3$ nm [18].

The chosen system, a PVDF/SMMA blend with the composition 3 : 2 wt/wt, was crystallized isothermally

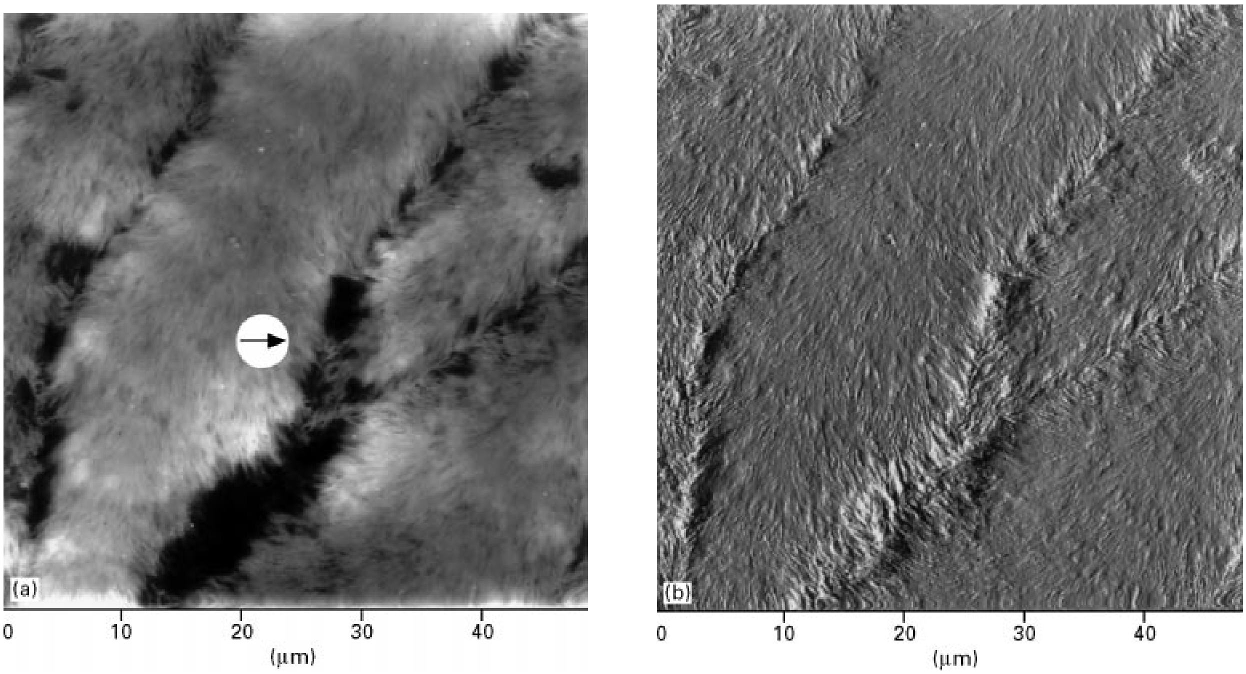

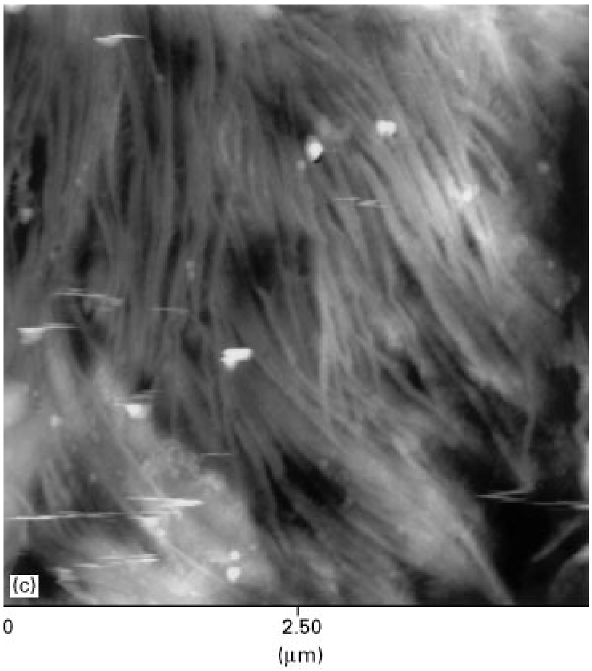

Figure 6 (a,b) Ends of twigs ("furry fox tails", arrow I, Fig. 5) : (a) AFM height (height variation, $\Delta h = 0\text{–}700$ nm); (b) AFM deflection; (c) magnification of lamellae (arrowed in (a), AFM height, $\Delta h = 0\text{–}300$ nm).

at 161 °C, i.e. at 18 K undercooling below the melting point of the α modification. These conditions lead to tree-like α crystals (Fig. 3). The morphology of the tree-like α and compact γ crystals in this blend is shown in Fig. 5. The positions specified by the arrows were studied by AFM.

While the crystals in Fig. 1 are isolated, growing in the melt, the crystals in Fig. 5 are in contact with each other and no longer grow. The blend is fully crystallized. The melt is clearly seen between the crystals and partly hidden inside the α spherulites. In this final stage of crystallization, the melt consists almost exclusively of the amorphous SMMA. It is, in terms of Fig. 2, a depletion zone that contains very little PVDF.

Ends of twigs at the outer front of the α crystal (arrow I, Fig. 5) are shown in Fig. 6. In the height image (Fig. 6a), the SMMA melt is dark because the SMMA was etched away. The height and the deflection (Fig. 6b) image show, in different types of contrast, that the crystalline PVDF twigs are covered by a fur of tiny lamellae. The growth of these surface lamellae is stopped by the SMMA melt. The highly magnified image in Fig. 6c reveals that the surface lamellae are poorly ordered. They grew fairly independently of each other, trying to collect PVDF in the depletion layer. The lamellae are $\cong 50$ nm thick, which is much more than the thickness of a single PVDF lamella in the crystallographic sense (Fig. 4). What is seen in Fig. 6c are stacks of a few correlated single lamellae.

The structure of a branch that splits up into twigs is illustrated in Fig. 7a. The image was taken not directly at, but just behind the front of the α crystal. Each twig is covered, on the outside, by a feathery surface layer of disordered lamellae. These surface layers are disordered, just like the ends shown in Fig. 6. But Fig. 7a demonstrates also that below their surface, the twigs are internally quite compact.

The spot indicated in Fig. 7a where the branch starts bifurcating into two twigs is resolved in high magnification in Fig. 7b. Surface lamellae of both twigs are beginning to grow in different directions. The disorder is reminiscent of Fig. 6c.

Fig. 7 solves the question of whether the tree-like PVDF spherulites are dendrites. They look like dendrites but the mechanism is different: in true dendrites, by definition, twigs are created on branches by crystallographic bifurcation. What this would mean for a polymer crystallizing in lamellar order is

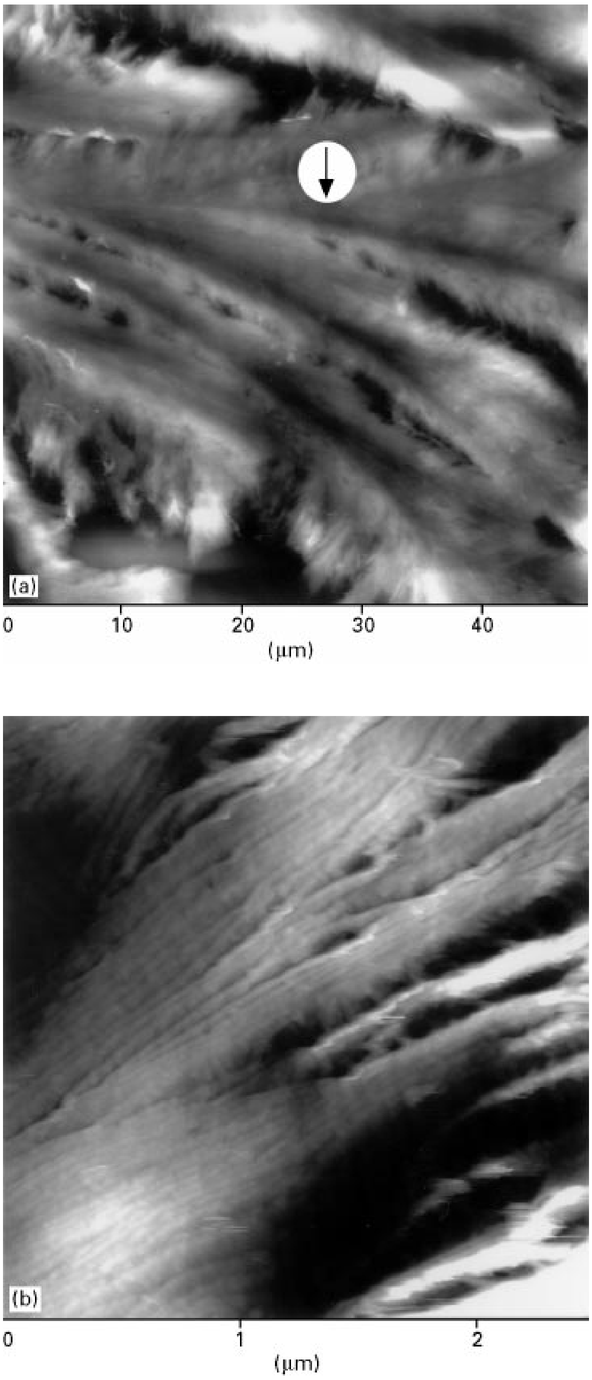

Figure 7 (a) Splitting branch near the crystalline front (growing from left to right, AFM height $\Delta h = 0$–1.7 μm); (b) surface lamellae of a bifurcating branch (arrowed in (a), AFM height, $\Delta h = 0$–200 nm).

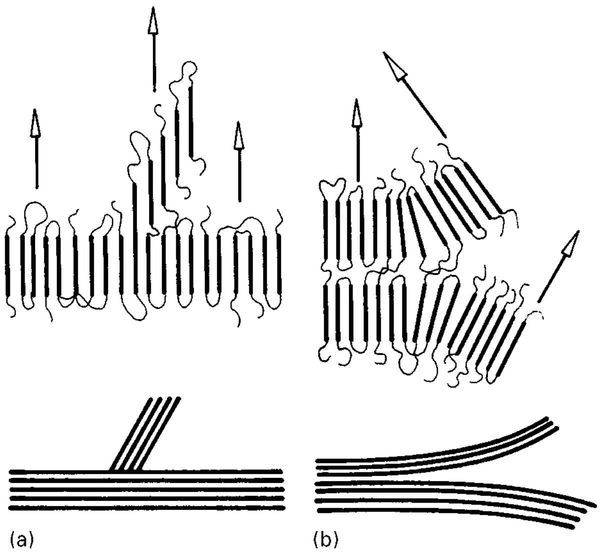

Figure 8 Bifurcations in the lamellar structure of a partly crystalline polymer: (a) dendritic, (b) tree-like; the arrows indicate the orientation of the polymer chains inside the lamellae.

indicated, schematically, in Fig. 8a. One lamella is split such that the chain orientation is preserved in the twig. This type of splitting process in polymers is too demanding to be competitive.

The dendritic architecture of the PVDF α crystals is rather the result of lamellar stacks drifting apart as observed in Fig. 7b and shown, schematically, in Fig. 8b. As discussed in detail elsewhere [1], the growth of branches and twigs in PVDF blend melts and similar systems is controlled by the PVDF gradient in the depletion layer. Branches and twigs grow simply into the direction of increasing PVDF concentration. Bifurcations, as in Fig. 8b, activate the crystallization because twigs that grow away from a branch cut rapidly through the depletion layer of that branch.

The tree-like PVDF α crystals are characterized, in the light micrograph in Fig. 5, by an obvious structure of branches, in the centre as well as in the outer spheres. Branching near the crystal front was confirmed by the AFM images in Figs 6 and 7. But surprisingly, AFM reflected no branching in the centre of the α crystals. The α core (arrow II, Fig. 5) in Fig. 9a looks, in fact, similar to the γ core (arrow III, Fig. 5) in Fig. 9b. Both consist of radially oriented lamellae in compact array. The lamellae are larger in the α and smaller in the γ crystal. Both cores contain tiny amorphous inclusions (well resolved in Fig. 9d) that are randomly distributed in the crystalline matrix. There is no evidence of a particular structure. To summarize, an open, disordered structure is observed only in the outskirts of the α crystals.

Another feature is resolved in Fig. 9a and c, as clearly as in Fig. 5: as in many other polymer spherulites [19–21], the α (but not the γ) crystals of PVDF feature a concentric ring pattern. The ring periodicity in both the optical micrograph (Fig. 4) and the AFM image (Fig. 7a) is approximately 7 ± 1 μm. The magnified deflection image in Fig. 9b shows part of one ring. This is due to lamellae that are viewed alternately edge-on and in-plane. The edge-on lamellae are etched more efficiently and therefore appear rougher in Fig. 9b than the smooth surface of the in-plane lamellae.

A transition from in-plane to edge-on lamellae is shown at high magnification in Fig. 10a. There is no gentle continuous twist of the lamellar orientation. The transition is quite abrupt, the orientation of the lamellar planes suddenly changing. This confirms other electron microscopic studies on ring patterns [21]. Some in-plane lamellae are magnified in Fig. 10b, together with a height profile. The steps are about

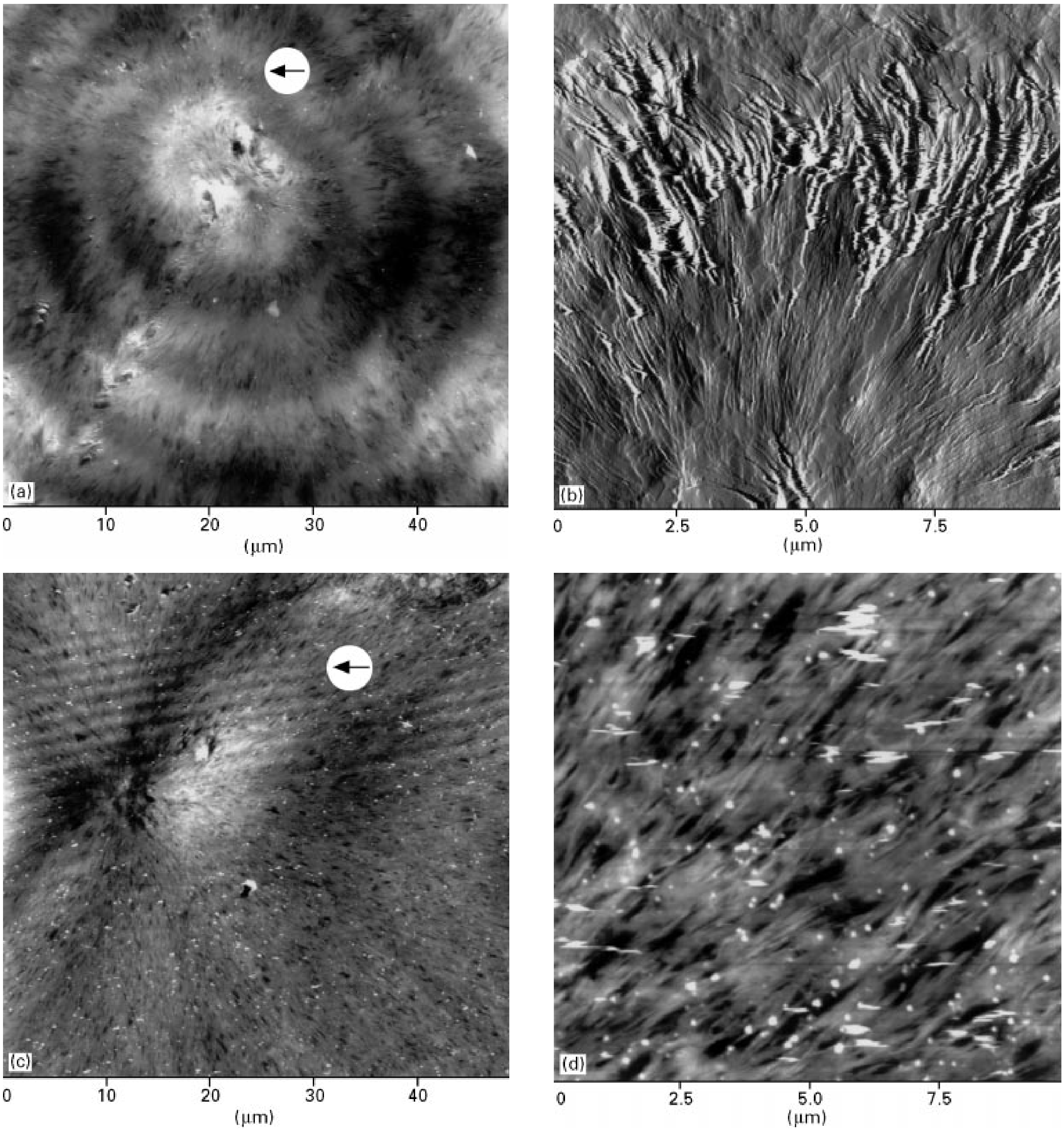

Figure 9 Centre and core of PVDF spherulites: (a) α crystal (arrow II, Fig. 5; AFM height, $\Delta h = 0$–400 nm) with (b) magnification (arrowed in (a), AFM deflection), (c) γ crystal (arrow III, Fig. 5; AFM height, $\Delta h = 0$–200 nm) with (d) magnification (arrowed in (c), AFM height, $\Delta h = 0$–100 nm). Dark spots are SMMA inclusions.

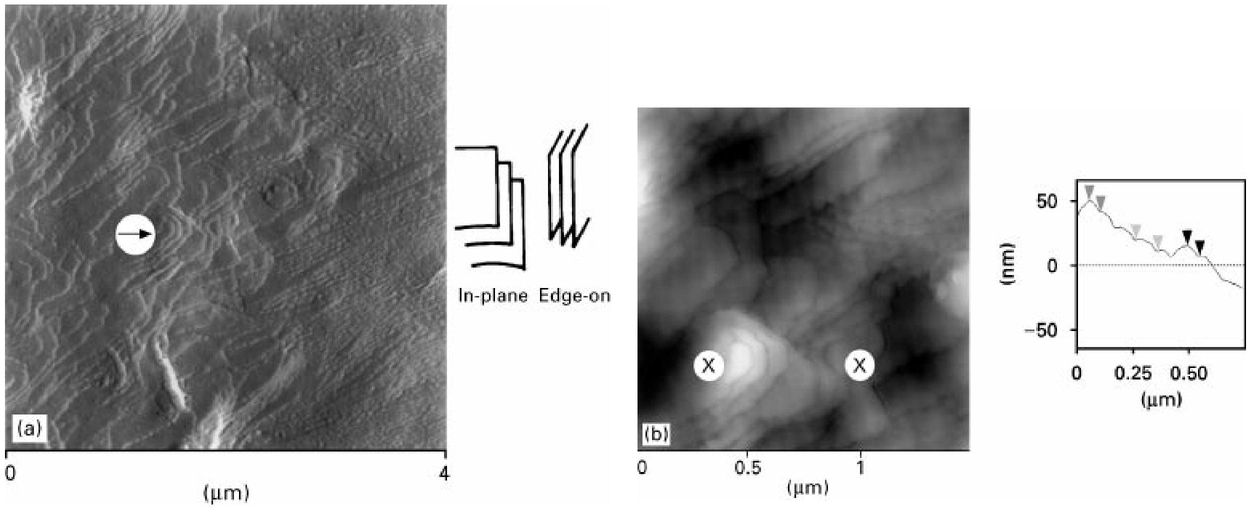

Figure 10 (a) Transition from an in-plane (left) to an edge-on (right) ring in the core of Fig. 9a (AFM deflection), with (b) magnification and height profile along the line X–X in (a) (AFM height, $\Delta h = 0$–130 nm).

7–9 nm in height, which corresponds to the thickness of the single α lamellae in Fig. 4.

Where two tree-like α crystals (or two branches of the same crystal) meet, the lamellae at the two fronts interpenetrate slightly, but they remain separated by an amorphous interphase of SMMA (Fig. 11). At spots where the contact between two crystals is more intimate, the lamellae fold back (Fig. 12).

4. Conclusion

The light microscopic analysis of PVDF crystals in homogeneous PVDF/SMMA blends reported earlier [1] concluded that the amorphous SMMA is ejected from the crystals which leads to particular morphologies, either to compact spherulites with an envelope of SMMA (Fig. 2a) or to tree-like spherulites with branches and twigs that are separated by SMMA (Fig. 2b). The tree-like architecture of the α crystals can be very open (Fig. 1) or somewhat more closed (Fig. 5).

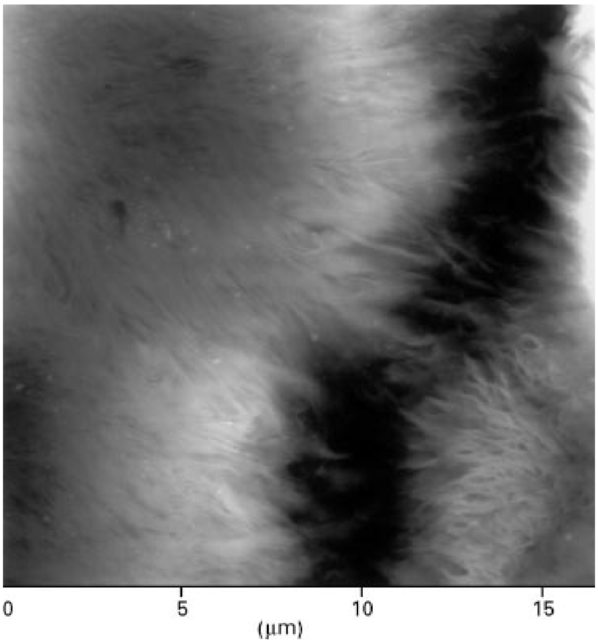

Figure 11 Fronts of two crystals in loose contact (AFM height, $\Delta h = 0$–1 μm).

The morphology in Fig. 5 is very characteristic for blends where the PVDF is completely crystallized: the γ crystals are featureless spheres while the α crystals are strongly structured, with bifurcating branches growing from the centre outwards to the front. The α crystals also feature a pattern of concentric rings. The submicroscopic AFM analysis of this morphology clarified the following points.

Cores: while the centre and the core of the α crystals appear branched, in the light micrograph in Fig. 5, the core as probed by AFM is rather compact, devoid of any superstructure (Fig. 9a). The cores of α and γ crystals look quite similar (Fig. 9a, c). They contain SMMA in small domains; however, these domains are randomly distributed (Fig. 9a, c, d).

Rings: the ring pattern in the α crystals (Fig. 9c) is caused by periodic changes of the orientation of the lamellae which was well resolved by AFM (Fig. 10). The transition is quite abrupt.

Outer spheres: in the outer spheres and at the front of the α crystals, branches and twigs are observed that form a tree-like architecture which is filled by amorphous SMMA (Figs 5 and 6). The branches and twigs consist of a compact inner strand that is covered by a loose surface layer of disordered lamellae.

Contacts: the SMMA melt usually prevents contact between the crystals (Figs 5 and 11). Surface lamellae of neighbouring α crystals touch only rarely. Where they do, the surface lamellae fold back on each other (Fig. 12).

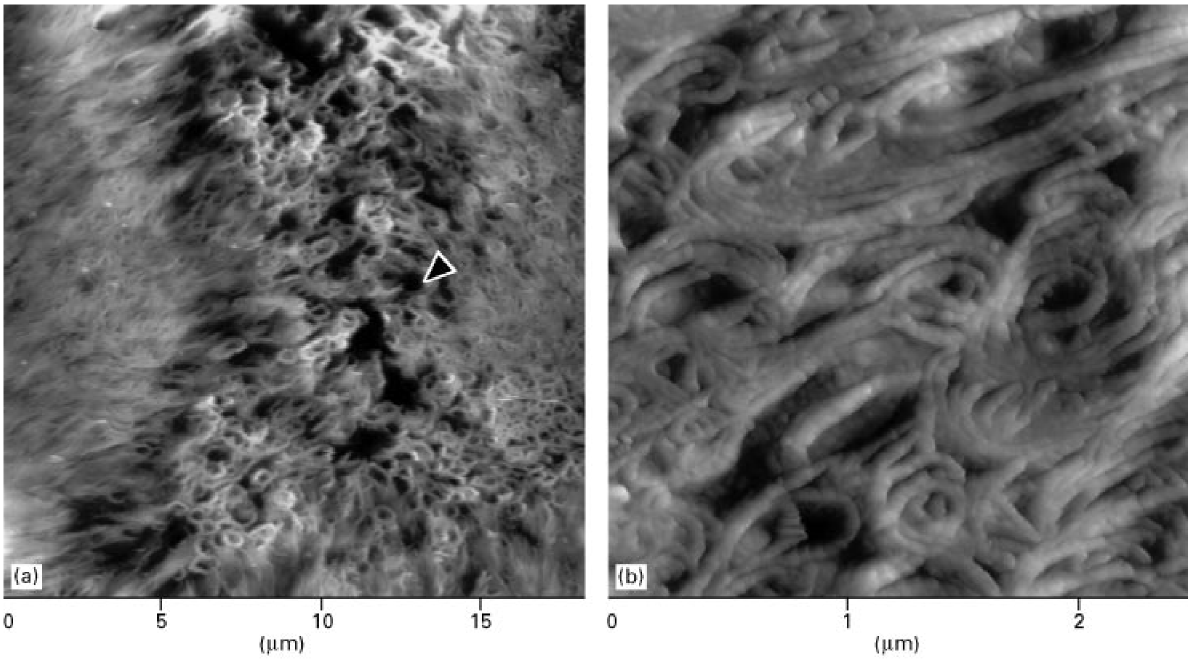

Figure 12 (a) Backfolding lamellae between two crystals in close contact (AFM height, $\Delta h = 0$–700 nm), and (b) magnification (arrowed in (a), AFM height, $\Delta h = 0$–150 nm).

In summary, this AFM study suggests that tree-like PVDF α crystals are less disordered than expected from light micrographs.

Acknowledgement

M. F. S. L. thanks the DAAD for financial support of her stay at the FMF.

References

1. D. BRAUN, M. JACOBS and G. P. HELLMANN, *Polymer* **35** (1994) 706.
2. B. S. MORRA and R. S. STEIN, *J. Polym. Sci. Phys.* **20** (1982) 2261.
3. R. M. BRIBER and F. KHOURY, *Polymer* **28** (1987) 38.
4. *Idem.*, *J. Polym. Sci. Phys.* **31** (1993) 1253.
5. H. D. KEITH and F. J. PADDEN, *J. Appl. Phys.* **34** (1963) 2409.
6. *Idem.*, *ibid.* **35** (1964) 1270.
7. D. T. GRUBB and K. W. CHOI, *ibid.* **52** (1981) 5908.
8. A. J. LOVINGER, *ibid.* **52** (1981) 5934.
9. W. M. PREST and D. J. LUCA, *ibid.* **46** (1975) 4136.
10. A. J. LOVINGER, *Polymer* **21** (1980) 1317.
11. *Idem.*, *J. Polym. Sci. Phys.* **18** (1980) 793.
12. *Idem.*, *Macromolecules* **14** (1981) 322.
13. G. BINNIG, C. QUATE and CH. GERBER, *Phys. Rev. Lett.* **56** (1986) 930.
14. R. WIESENDANGER and H.-J. GÜNTHERODT (Eds), "Scanning Tunneling Microscopy I, II, III" (Springer, Heidelberg, 1992/93).
15. N. A. BURNHAM and R. J. COLTON, in "Scanning Tunneling Microscopy and Spectroscopy", edited by D. Bonnel (VCH, New York, 1993) p. 191.
16. A. WAWKUSCHEWSKI, K. CRÄMER, H. -J. CANTOW and S. N. MAGONOV, *Ultramicroscopy* **58** (1995) 185.
17. K. OKUDA, T. YOSHIDA, M. SUGITA and M. ASAHINA, *J. Polym. Sci. B* **5** (1967) 465.
18. J. C. CANALDA, TH. HOFFMANN and J. MARTINEZ-SALAZAR, *Polymer* **36** (1995) 981.
19. H. D. KEITH and F. J. PADDEN, *J. Polym. Sci.* **39** (1959) 101.
20. *Idem.*, *ibid.* **39** (1959) 123.
21. D. C. BASSETT and A. M. HODGE, *Proc. R. Soc. Lond. A* **377** (1981) 61.
22. T. A. WITTEN, and L. M. SANDER, *Phys. Rev. Lett.* **47** (1981) 1400.
23. *Idem.*, *Phys. Rev. B* **27** (1983) 5686.

Received 28 May
and accepted 5 December 1997